Spectrochimica Acta Part A 79 (2011) 1050–1056

Contents lists available at ScienceDirect

Spectrochimica Acta Part A: Molecular and Biomolecular Spectroscopy

journal homepage: www.elsevier.com/locate/saa

Synthesis and DNA binding studies of Ni(II), Co(II), Cu(II) and Zn(II) metal complexes of N^1,N^5-bis[pyridine-2-methylene]-thiocarbohydrazone Schiff-base ligand

A.D. Tiwari [a], A.K. Mishra [b,*], S.B. Mishra [a], B.B. Mamba [a], B. Maji [c], S. Bhattacharya [c]

[a] Department of Chemical Technology, University of Johannesburg, P.O. Box 17011, Doornfontein 2028, South Africa
[b] UJ Nanomaterials Science Research Group, Department of Chemical Technology, University of Johannesburg, P.O. Box 17011, Doornfontein 2028, South Africa
[c] Department of Organic Chemistry, Indian Institute of Sciences, Bangalore, India

ARTICLE INFO

Article history:
Received 17 January 2011
Received in revised form 16 March 2011
Accepted 13 April 2011

Keywords:
Synthesis
Metal complex
Thiocarbohydrazone
DNA interaction
Schiff-base

ABSTRACT

The thiocarbohydrazone Schiff-base ligand with a nitrogen and sulphur donor was synthesized through condensation of pyridine-2-carbaldehyde and thiocarbohydrazide. Schiff-base ligands have the ability to conjugate with metal salts. A series of metal complexes with a general formula $[MCl_2(H_2L)]\cdot nH_2O$ (M=Ni, Co, Cu and Zn) were synthesized by forming complexes of the N^1,N^5-bis[pyridine-2-methylene]-thiocarbohydrazone (H_2L) Schiff-base ligand. These metal complexes and ligand were characterized by using ultraviolet–visible (UV–Vis), Fourier Transform Infrared (FT-IR), ^1H and ^{13}C NMR spectroscopy and mass spectroscopy, physicochemical characterization, CHNS and conductivity. The biological activity of the synthesized ligand was investigated by using *Escherichia coli* DNA as target. The DNA interaction of the synthesized ligand and complexes on *E. coli* plasmid DNA was investigated in the aqueous medium by UV–Vis spectroscopy and the binding constant (K_b) was calculated. The DNA binding studies showed that the metal complexes had an improved interaction due to trans-geometrical isomers of the complexes than ligand isomers in cis-positions.

1. Introduction

Schiff-base ligands are potential anti-cancer, anti-bacterial and anti-viral agents and this activity tends to increase in metal(II) Schiff-base complexes [1,2]. The cleavage of plasmid DNA by square planar nickel (salen) [bis-(salicylidene) ethylenediamine] under the influence of magnesium monoperoxyphthalic acid (MPPA) or iodosylbenzene has been well-reported [3]. The stereospecific transformation of Cu(II) complexes as groove binder and intercalative mode of binding of the complex to the DNA was studied by electron spin resonance (ESR) [4]. Bhattacharya et al. also reported the spontaneous cleavage of DNA under ambient aerobic conditions by a new water-soluble Co–salen complex [5]. The introduction of the divalent metal cation into the DNA structure modulates its function [6]. The mechanism of action of metal complexes as anticancer agents is such that it binds with the DNA of tumour cells resulting in the inhibition of its growth. An understanding of DNA binding mode and cleavage is needed to develop new and efficient antitumor drugs as their effectiveness depends on the binding mode and affinity towards the DNA [7,8]. Furthermore, the efficiency of these drugs also depends upon the structure activity relationship (SAR) with DNA that directly influences the drug-action mechanism under physiological conditions [9–11]. As determined by physical and biochemical methods, the principle mode of DNA binding is the intercalation of the metal complex between the base pair within a duplex DNA [12,13]. DNA offers a variety of binding sites and binding modes for non-covalent interactions with small molecules. The complexes can bind to DNA in non-covalent mode such as electrostatic, intercalative and groove binding [14,15]. The cationic metal complexes possess planar aromatic ligands in between adjacent base pairs within a duplex DNA [16–19].

The development of metal complexes as diagnostic or therapeutic agents requires techniques that can rapidly and accurately provide information about the effects of structural alterations on DNA selectivity and affinity. The non-covalent bonding of metal complexes with DNA has resulted in various applications such as synthetic restriction enzymes [20], DNA repair agents [21], development of selective probes of DNA structure [22], and artificial regulators of gene expression [23].

In the study reported in this article we synthesized Schiff-base N^1,N^5-bis[pyridine-2-methylene]-thiocarbohydrazone ligand. The metal(II) Schiff-base complexes using Ni(II), Co(II), Cu(II), and Zn(II) metals salts were prepared using the Schiff-base lig-

* Corresponding author. Tel.: +27 11 559 6180; fax: +27 11 559 6425.
E-mail address: amishra@uj.ac.za (A.K. Mishra).

1386-1425/$ – see front matter © 2011 Elsevier B.V. All rights reserved.
doi:10.1016/j.saa.2011.04.018

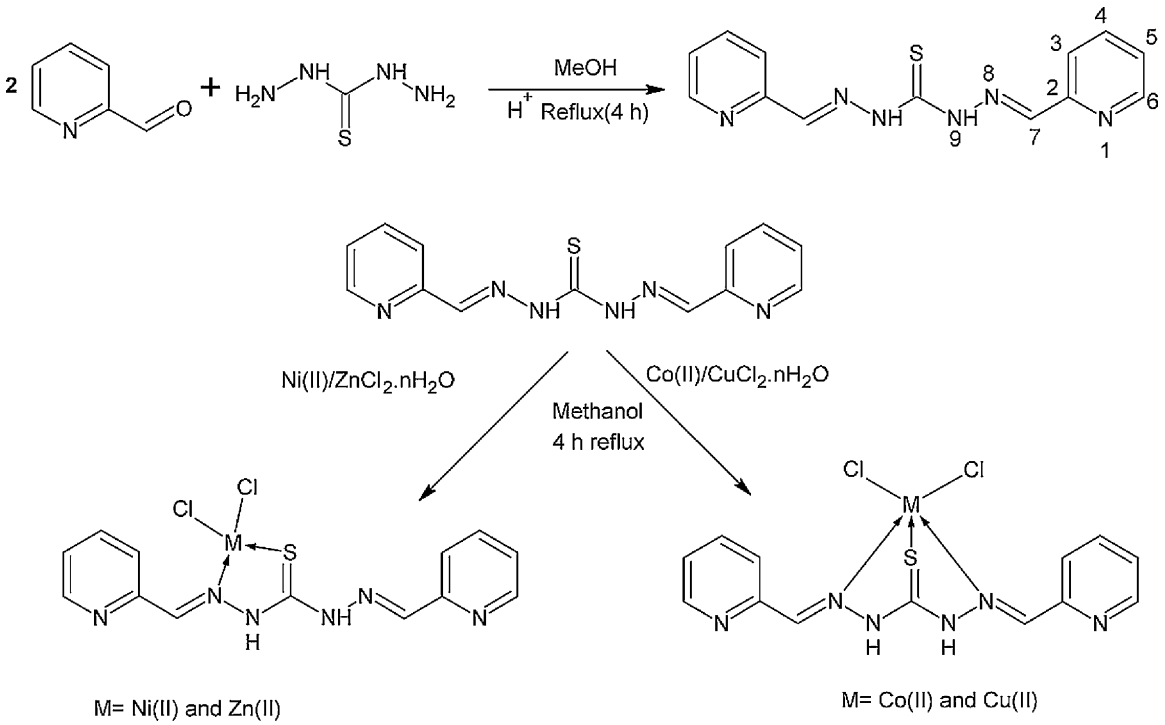

Scheme 1. Synthesis of the metal(II) Schiff-base complex methodology.

and. The ligand and the respective metal complexes were characterized by means of physical and spectral analyses. The complexes were used to study the DNA binding mechanism and binding constants in an aqueous medium by absorption spectroscopy.

2. Experimental

2.1. Materials

Plasmid genomic DNA was extracted from *Escherichia coli* as per the earlier reported methods [24]. The metal salts $ZnCl_2$, $CuCl_2{\cdot}2H_2O$, $NiCl_2{\cdot}6H_2O$, and $CoCl_2{\cdot}6H_2O$ were purchased from Merck, South Africa. Thiocarbohydrazide and pyridine-2-aldehyde were purchased (synthetic grade) from Sigma–Aldrich and Merck, South Africa, respectively. All the solvents (AR grade) used in the synthesis and analysis were procured from Merck, South Africa and used without any further purification.

2.2. Physical and spectral measurements

Melting points were measured using electrothermal digital melting point apparatus and molar conductivity was measured on the Crison EC Meter Basic 30+. The entire mass spectrums were obtained using a Waters Micromass Q-TOF Spectrometer. Elemental analysis (CHNS/O) was conducted on an elemental Varian analyzer. FT-IR spectra were recorded on the MIDAC FT-IR (4000 Model) in the range of 400–4000 cm^{-1} using a KBr disc. UV–Vis Spectra were recorded on the Varian Cary 50 Spectrophotometer (range 200–900 nm) using methanol as a solvent. Metal complex–DNA titration studies were performed on a Perkin Elmer Lambda-35 UV-Vis Spectrophotometer at room temperature, and deionised water was used. The ^{13}C and ^{1}H NMR Spectra were recorded using Varian Gemini-2000 NMR-300 with d_6-DMSO being the solvent containing tetra-methyl-silane (TMS) as the internal standard.

2.3. Synthesis

The Schiff-base ligand was prepared using a previously reported method and synthesis of the metal(II) Schiff-base complexes is depicted in Scheme 1 [25,26].

2.3.1. Synthesis of N^1,N^5 bis(pyridine-2-methylidene)-thiocarbohydrazone (H_2L)

Pyridine-2-aldehyde (10 mmol, 0.94 mL) was added to the thiocarbohydrazide (5 mmol, 0.536 g) in hot methanolic solution of Schiff-base with 1 mL HCl (0.1 N). The mixture was heated to reflux in the water bath for 4 h (Scheme 1). The pale yellow precipitate was formed by ice cooling. This (precipitate) was filtered off, washed with methanol and petroleum ether. Re-crystallization was carried out in methanol and a yellow amorphous compound was obtained, which was subsequently dried over anhydrous $CaCl_2$ under vacuum (m.p. 200 °C, yield 80%).

2.3.2. Synthesis of metal complexes

All the metal complexes were synthesized by adding the methanolic solution of metal(II) salts (0.5 mmol) to the hot homogeneous solution of the ligand (0.5 mmol) in the methanol. The mixture of the metal and the ligand was heated to reflux with constant stirring in a water bath for 4 h (Scheme 1). At room temperature, the product was filtered off. The obtained products were dried over anhydrous $CaCl_2$ under vacuum.

2.4. DNA binding studies

Stock solutions (500 μM) of the metal(II) Schiff-base complexes were prepared in the DMSO and then diluted using deionised water. All the experiments involving the interaction of the complexes with plasmid DNA were carried out in deionised water containing Tris–HCl buffer solution (0.6 M HCl) at room temperature and 50 mM NaCl, and adjusted to pH = 7.32. Aliquots of 5 μL plasmid DNA (19.1 ng/μL and 23.1 ng/μL) were added continuously while

Table 1
Physical properties of the ligand (H_2L) and its metal complexes.

Compound	Colour	mp (°C)	Yield (%)	Conductivity μS/cm (10^{-3})
$(H_2L)C_{13}H_{12}N_6S$	Yellow	200	75	–
$[(H_2L)NiCl_2]\cdot 3H_2O$ $C_{13}H_{14}N_6OSNiCl_2$	Red brown	363	79	185.1
$[(H_2L)CoCl_2]\cdot 3H_2O$ $C_{13}H_{16}N_6O_2SCoCl_2$	Dark black red	294	67	135.7
$[(H_2L)CuCl_2]\cdot 2H_2O$ $C_{13}H_{14}N_6OSCuCl_2$	Dark green	320	85	149.2
$[(H_2L)ZnCl_2]\cdot 2H_2O$ $C_{13}H_{14}N_6OSZnCl_2$	Lemon yellow	263	75	147.6

Table 2
CHNS/O and mass spectral data for ligand and metal complexes.

Compound	Mass	C% obs. (cald)	H% obs. (cald)	N% obs. (cald)	S% obs. (cald)	Cl% obs. (cald)	O% obs. (cald)	M% obs. (cald)
H_2L	307	54.87	4.34	27.98	11.50	–	–	–
$C_{13}H_{12}N_6S$	[M+Na]	(54.91)	(4.25)	(29.56)	(11.28)			
$[(H_2L)NiCl_2]\cdot 3H_2O$	341	32.41	3.65	16.87	5.89	(15.15)	(10.26)	(12.54)
$C_{13}H_{12}N_6SNiCl_2\cdot 3H_2O$	[M−2Cl−H]	(33.36)	(3.88)	(17.96)	(6.85)			
$[(H_2L)CoCl_2]\cdot 3H_2O$	413	31.83	3.79	16.61	6.85	(15.14)	(10.25)	(12.59)
$C_{13}H_{12}N_6SCoCl_2\cdot 3H_2O$	[M−H]	(33.35)	(3.87)	(17.95)	(7.21)			
$[(H_2L)CuCl_2]\cdot 2H_2O$	346	34.03	3.51	17.34	7.68	(15.66)	(7.07)	(14.03)
$C_{13}H_{12}N_6SCuCl_2\cdot 2H_2O$	[M−2Cl]	(34.48)	(3.12)	(18.56)	(7.08)			
$[(H_2L)ZnCl_2]\cdot 2H_2O$		33.98	2.94	17.67	7.17	(15.53)	(7.01)	(14.32)
$C_{13}H_{12}N_6SZnCl_2\cdot 2H_2O$		(34.19)	(3.53)	(18.40)	(7.02)			

titrating. DNA and compound solutions were allowed to incubate for 10 min at room temperature. Absorption spectrums were recorded. A fixed amount of the compound, i.e., 500 μL (50 μM), was titrated with increasing amounts of DNA, over a DNA concentration range of 0–70 μM.

3. Result and discussion

All the metal complexes were synthesised with an equimolar ratio of ligand and metal salts in methanol. The ligand (H_2L) was synthesized by the condensation of diamine and aldehyde, and characterized by UV–Vis, IR, mass spectra, ^1H and ^{13}C NMR and physical techniques like CHNS/O. The complexes formed were $[(H_2L)NiCl_2]\cdot 3H_2O$ (1), $[(H_2L)CoCl_2]\cdot 3H_2O$ (2), $[(H_2L)CuCl_2]\cdot 2H_2O$ (3) and $[(H_2L)ZnCl_2]\cdot 2H_2O$ (4). Due to the amorphous nature of the complexes, all the efforts were in vain to develop the crystal. The binding and coordination modes of the ligand and its metal complexes were determined by spectral data studies.

Table 1 represents the preliminary observations of the synthesized compounds with respect to colour, melting point (mp), yield and conductivity. The complexes are insoluble in water; however, they are sparingly soluble in DMSO. The complexes show low molar conductivity indicating their non-electrolytic behaviour [27]. Elemental analysis of the compounds was conducted and the findings are given in Table 2.

3.1. Spectral characterization of compounds synthesized

3.1.1. UV–Vis spectroscopy

The UV–Vis spectral data of the ligand and its metal complexes are given in Table 3. Two absorption bands were observed for the ligand corresponding to $n \rightarrow \pi$ and $n \rightarrow \sigma^*$ bands at 340 nm and 275 nm for azomethine (HC=N) and (N–N) chromophores, respectively.

The absorption spectra of the Ni(II) complex bands were observed at 362 nm which is a higher wavelength shifting of the azomethine band of $n \rightarrow \pi^*$ showing the coordination of the Ni(II) with (HC=N). New bands in the complex appeared at ~418 nm which is the charge transfer band for the S → Ni(II) and the absorption band at 485 nm is assigned to the d–d transition band $^4T_{1g}(F) \rightarrow {}^4A_{2g}(F)$. The Ni(II) coordination sphere completes its five-coordination by two nitrogen ions, one sulphur ion and two chloride ions. From the above spectral data complex the sphere seems to prefer the distorted tetrahedral geometry [28].

The Co(II) complex showed the $^4T_{1g}(F) \rightarrow {}^4A_{2g}(F)$ d–d transition bands at 529 nm. The 10 nm shift to a higher wavelength was attributed to the azomethine band observed at 350 nm as a result of the coordination with C=N in the Co(II) complex. The charge transfer band for the S → Co(II) could be seen at 303 nm and there was also a 20 nm lower wavelength shift observed in the N–N chromophore bands of 275 nm of free ligand which was observed at 255 nm. The Co(II) metal is coordinated to three donor sites of the ligand and has assumed a square pyramidal geometry [28].

The UV–Vis spectra of the Cu(II) complex showed peaks at 355 nm and 425 nm. The azomethine band was shifted to higher wavelength in the Cu(II) complex. The new band was at 425 nm assigned to the S → Cu(II) showing the coordination. The C=N and C=S groups are coordination sites of the ligand in Cu(II) complex. The ligand is coordinated to copper by the two C=N and one C=S, and two chloride ions from the metal salts making a five coordination sphere around the Cu(II). From the above data and lack of the characteristic peak of Cu(II) at around ~800 nm the trigonal bipyramidal geometry is proposed for the Cu(II) complex [28,29].

Table 3
UV–Vis Spectral data (nm) for H_2L and its metal complexes (methanol 200–900 nm).

Compound	(HC=N) $n \rightarrow \pi^*$ (nm)	N–N $n \rightarrow \sigma^*$ (nm)	Intra-ligand charge transfer (nm)	$d \rightarrow d$ (nm)
H_2L	340 (s)	275 (w)	–	–
$[(H_2L)NiCl_2]\cdot H_2O$	362 (s)	271 (w)	418 (m)	485 (w)
$[(H_2L)CoCl_2]\cdot 2H_2O$	350 (s)	255 (w)	303 (m)	529 (w)
$[(H_2L)CuCl_2\cdot 2H_2O]\cdot H_2O$	355 (s)	260 (w)	–	425 (w)
$[(H_2L)ZnCl_2]\cdot 2H_2O$	350 (s)	275 (w)	218 (m)	–

s: small, w: weak, m: medium.

Table 4
Characteristic IR bands of the H_2L and its metal complexes (in KBr disc 400–4000 cm^{-1}).

Compound	ν(N–H)	ν(HC=N)	ν(N–N)	ν(H_2O)	ν(C=S)	ν(S=C–NH)	ν(M–N)
H_2L	3130	1609	1111	3468	783	1529–1111	–
$[(H_2L)NiCl_2]\cdot H_2O$	3094	1615	1147	3407	764	1519–1147	511
$[(H_2L)CoCl_2]\cdot 2H_2O$	3090	1612	1141	3408	766	1521–1091	503
$[(H_2L)CuCl_2\cdot 2H_2O]\cdot H_2O$	3102	1618	1111	3442	768	1563–1010	508
$[(H_2L)ZnCl_2]\cdot 2H_2O$	3085	1622	1147	3444	777	1541–1147	515

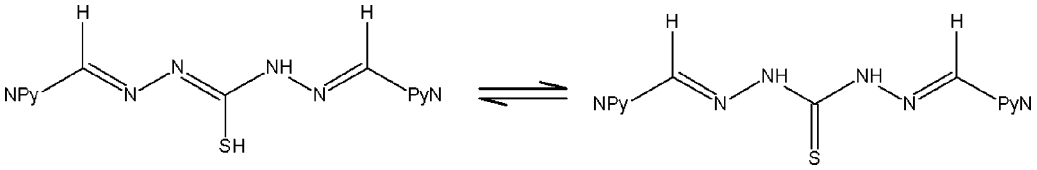

Fig. 1. Tautomeric form and hyper-conjugation behaviour of the ligands.

Table 5
^1H NMR (300 MHz) spectral data (ppm) for H_2L ligand and its metal complexes (DMSO-d_6).

Compound	^3CH	^4CH	^5CH	^6CH	$^7HC=N$	^9NH
H_2L	7.85 (d)	7.44 (dd)	7.90 (dd)	8.64 (d)	8.26 (s)	8.87 (s)
$[(H_2L)NiCl_2]\cdot H_2O$	7.84 (d)	7.47 (dd)	8.05 (dd)	8.59 (d)	8.96 (s)	–
$[(H_2L)CoCl_2]\cdot 2H_2O$	–	–	–	–	–	–
$[(H_2L)CuCl_2\cdot 2H_2O]\cdot H_2O$	–	–	–	–	–	–
$[(H_2L)ZnCl_2]\cdot 2H_2O$	7.83 (d)	7.47 (dd)	8.12 (dd)	8.63 (d)	8.35 (s)	8.84 (s)

d: doublet, and s: singlet.

The UV–Vis spectrum of the Zn(II) complex is dominated by the free ligand absorption bands. A red shift of 15 nm was observed in the complex confirming the coordination of the azomethine group with Zn(II) ion. An inter-ligand charge transfer band was observed at 218 nm and the metal to ligand charge transfer band was observed at 470 nm. The zinc metal ion is coordinated by two C=N from the ligand and two chloride ions from the metal salts making up a four coordination sphere for the tetrahedral coordinated geometry [28].

3.1.2. Infrared (IR) spectroscopy

Spectral analysis data are given in Table 4 for the ligand and its metal complexes. The infrared spectral data of the Schiff-base ligand show the characteristic peaks for the functional groups like –CH=N–, C=S, N–H, and N–N group at 1609 cm^{-1}, 783 cm^{-1}, 3130 cm^{-1}, and 1111 cm^{-1}, respectively, and thioamide I, II, III, IV vibrations at 1529 cm^{-1}, 1429 cm^{-1}, 1236 cm^{-1} and 1111 cm^{-1}, respectively, were observed in the ligand [27–30]. The IR spectra of the metal(II) Schiff-base complexes show a broad band at ~3440 cm^{-1} for the ν(OH) group of coordinated water. The ν(N–H) group vibration bands in all the complexes shifted or even disappeared or appeared to be very weak due to resonance and hyper conjugation between the C=S and C=N with NH. The azomethine ν(HC=N) vibration band in the complex shifted to a higher frequency due to the increase in bond length through coordination with the metal(II) centre.

In the Co(II), Ni(II), Cu(II) and Zn(II) complexes there were ~40 cm^{-1} shifts to a lower frequency, confirming the coordination to the nitrogen atom with Ni(II) in the complex. The ν(C=S) vibration in the complex (Table 4) shifted to a lower frequency in the metal complex due to the coordination of the sulphur to the Ni(II) metal centre. In the Co(II) complex no shift was observed for the N–N peak data in the complex, suggesting that the bond was not involved in the coordination (Fig. 1).

The vibration of the thioamide IV bands also shifted with respect to their participation in the coordination sphere of the metal(II) ions. Their new band appeared in the complexes due to the ν(M–N) vibration, suggesting the bonding between the nitrogen and metal(II) ion.

3.1.3. ^1H and ^{13}C NMR spectroscopy

^1H NMR spectral data of the ligand in d_6-DMSO (Table 5) confirm the proposed structure elucidation of the ligand (Scheme 1). The characteristic peak data of ^1H NMR for the ligand and its complexes are given in Table 5. The NMR spectra for the Co(II) and Cu(II) complexes could not be recorded due to the paramagnetic property of metal complexes. There was strong evidence of Schiff-base ligand synthesis of the N^1,N^5-bis-(pyridine-2-methylene) thiocarbohydrazone (H_2L) [30]. The signal at the 8.26 ppm(s) was assigned to the azomethine (HC=N) proton. The NH proton is assigned at the 8.87 ppm(s). The aromatic region signal was observed from 7.44 ppm to 8.64 ppm (Table 5). In the Ni(II) complexes, the NH pro-

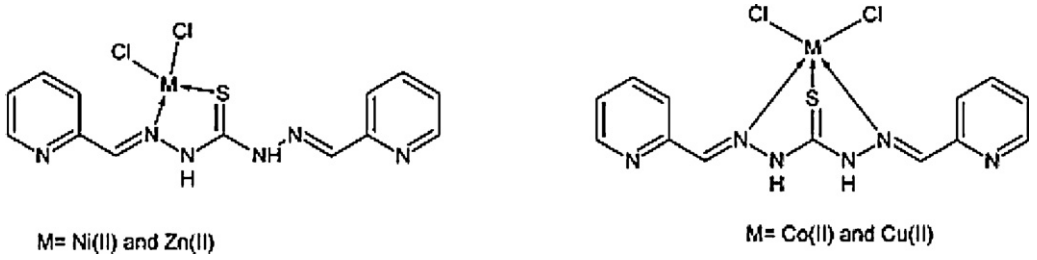

Fig. 2. Proposed structure for the metal complexes.

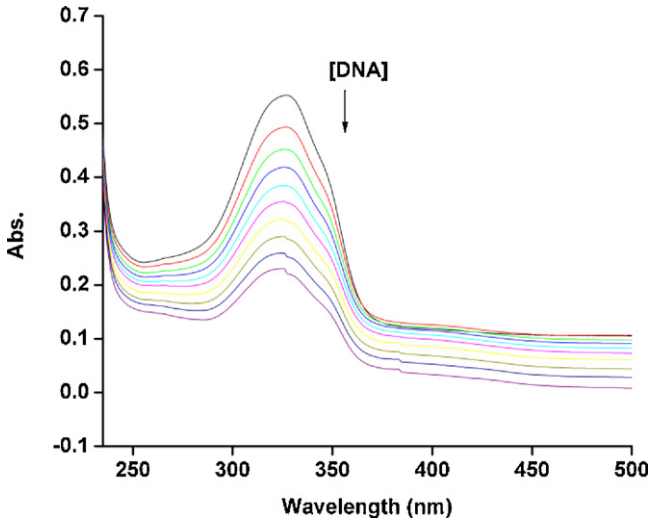

Fig. 3. (H_2L), ligand–DNA titration graph of 50 μM of ligand in 500 μL of Tris–HCl buffer, 50 mM NaCl, pH 7.32 with *E. coli* plasmid DNA (19.1 ng/μL). Arrows show the absorption change upon increasing DNA concentration.

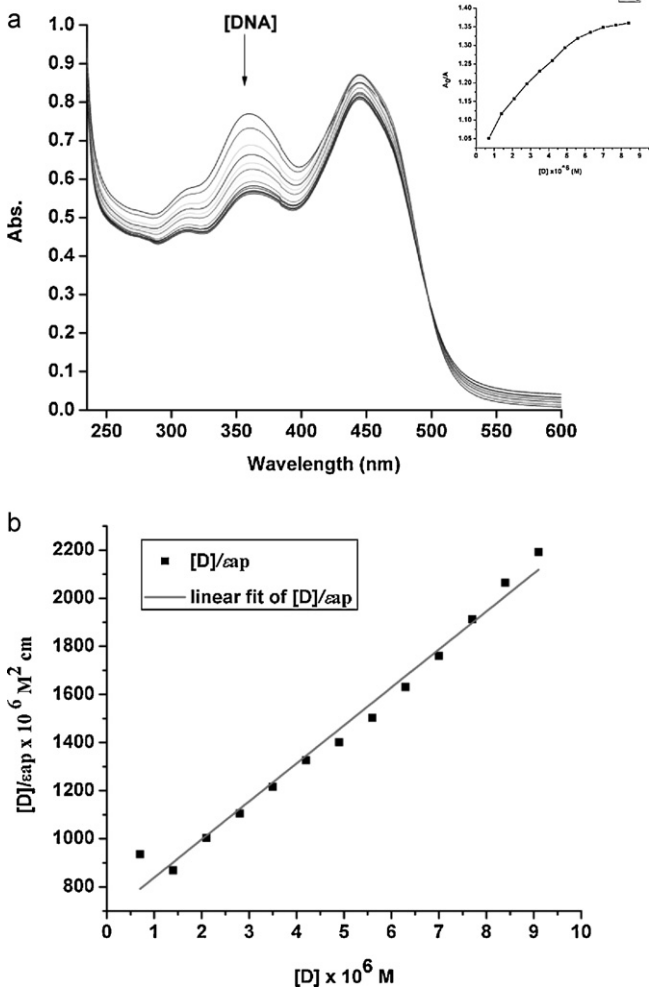

Fig. 4. (a) (1), Ni(II)L_1–DNA titration graph of 50 μM of complex in 500 μL of Tris–HCl buffer, 50 mM NaCl, pH 7.32 with *E. coli* plasmid DNA (23.1 ng/μL);(complex-DNA saturation curve is given in insert). (b) Ni(II)L_1–DNA: half-reciprocal plot of D/ε_{ap} vs. D. The binding constant, K_b = (slope/intercept) × 10^6 = 2.3×10^5 M^{-1}. Arrows show the absorption change upon increasing DNA concentration.

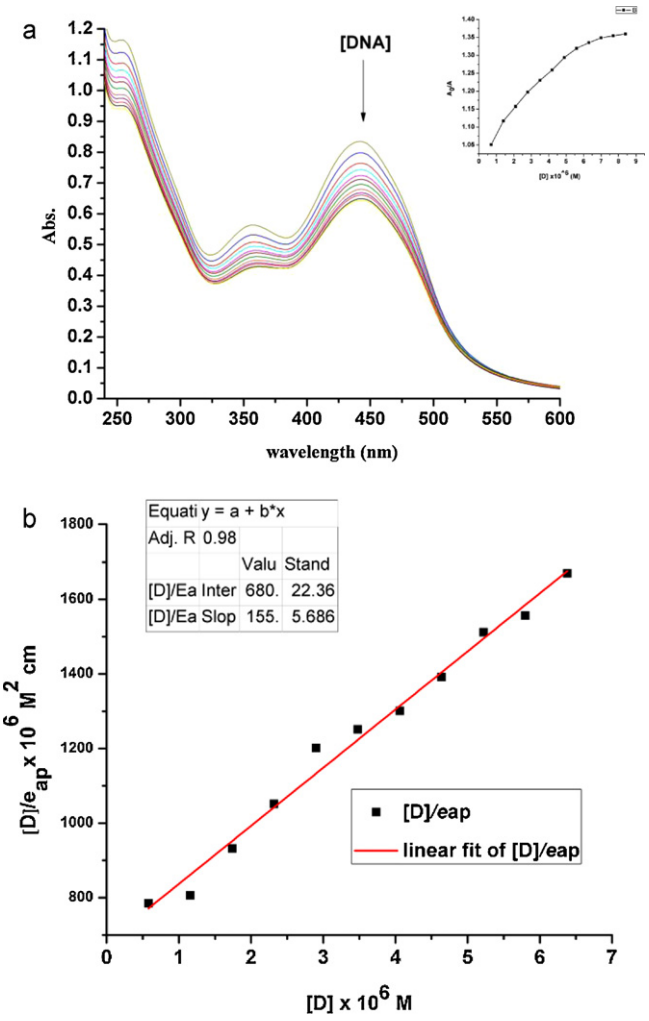

Fig. 5. (a) Co(II)L_1–DNA titration graph of 50 μM of complex in 500 μL of Tris–HCl buffer, 50 mM NaCl, pH 7.32 with *E. coli* plasmid DNA (19.1 ng/μL); (saturation curve is given in insert). (b): Co(II)L_1–DNA: half-reciprocal plot of D/ε_{ap} vs. D. The binding constant, K_b = (slope/intercept) × 10^6 = 2.1×10^5 M^{-1}.

ton disappeared in deuterium exchange showing the involvement of the NH in the bonding. However, in the case of the Zn(II) complexes, the NH proton does not disappear in deuterium exchange due to the bonding with –C=N.

Since the aromatic group did not participate directly in the coordination there was a very small shift in that region but the azomethine proton shifted down the field due to the positive centre of the metal coordination with the ligand HC=N group (Scheme 1 and Fig. 2). From Fig. 2 the tautomeric effect was explained by the ^{13}C NMR spectra. Two types of carbon peaks were observed for the C=S and C–SH at 175.48 cm^{-1} and 176.73 cm^{-1}, respectively. Other peaks are also given in Table 6 and in Scheme 1 [31,32].

3.2. Electronic absorption titration of DNA-binding studies

UV–Vis absorption spectroscopy is one of the most commonly used techniques for investigation of the binding mode of metal complexes to DNA [34]. Absorption titrations were carried out by keeping the concentration of the probe constant while adding a concentrated solution of *E. coli* genomic DNA. The saturation in hypochromism was observed. The saturation in hypochromism is quantitative in most of the cases which is shown by plotting the A_0/A vs. [DNA] where A_0 and A are the absorption intensities of the

Table 6
^{13}C NMR (75 MHz) spectral data (ppm) for the ligand (DMSO-d_6).

Ligand/gp	C=S	C–SH	HC=N	HS–C=N	Py^2C=N	Py^3C	Py^5C	Py^6C=N	Py^4C
H_2L	175.48	176.73	151.32	152.72	149.71	124.37	126.59	139.32	137.02

individual metal-complexes in the absence and presence of various concentrations of DNA. The binding constants were calculated from the following equation:

$$\frac{D}{\Delta\varepsilon_{ap}} = \frac{D}{\Delta\varepsilon} + \frac{1}{\Delta\varepsilon \times K} \quad (1)$$

where D is the concentration of DNA in the base molarity, $\Delta\varepsilon_{ap} = |\varepsilon_a - \varepsilon_f|$, and $\Delta\varepsilon = |\varepsilon_b - \varepsilon_f|$, where ε_b and ε_f are respective extinction coefficients of the ligand in the presence and absence of DNA.

The apparent extinction coefficient ε_{ap} was obtained by calculating A_{obs}/[ligand] where A_{obs} was the observed absorbance. The data were fitted to Eq. (1) to obtain a straight line with a slope = $1/\Delta\varepsilon$ and y-intercept = $1/(\Delta\varepsilon \times K)$. The binding constants K were determined from the ratio of the slope to the y-intercept [33,35].

The DNA–ligand titration absorption curve in Fig. 3 shows that there is no interaction between the DNA and the ligand because there is no charge on the ligand and even the ligand is planar so it cannot bind in any possible way to the DNA. The absorption reduces every time after addition of the DNA due to the dilution factor.

The titration absorption curve for the DNA binding activity with the Ni(II)L_1 complex is shown in Fig. 4 showing the best interaction with DNA among all the metal complexes. They interact more strongly with DNA and they have a higher binding constant than the other complexes, due to the possible geometry of the Ni(II) complex of the distorted tetrahedral. The best result for the Ni(II) complex was shown towards plasmid DNA by UV–Vis spectroscopy. There is a hypochromism effect as well as a red-shift at $\lambda = 368$ nm ($\Delta\lambda = 4.9$ nm) with a binding constant of 2.3×10^5 M^{-1} and having isosbestic point at $\lambda = 498.2$. The presence of isosbestic point in this titration suggests that there exist chemical equilibrium between the bound and free metal complexes or the ligand with no spectroscopic detectable intermediate states in the presence of DNA. Strong hypochromism and spectral broadening in absorption intensities indicates intense interaction between the electronic states of

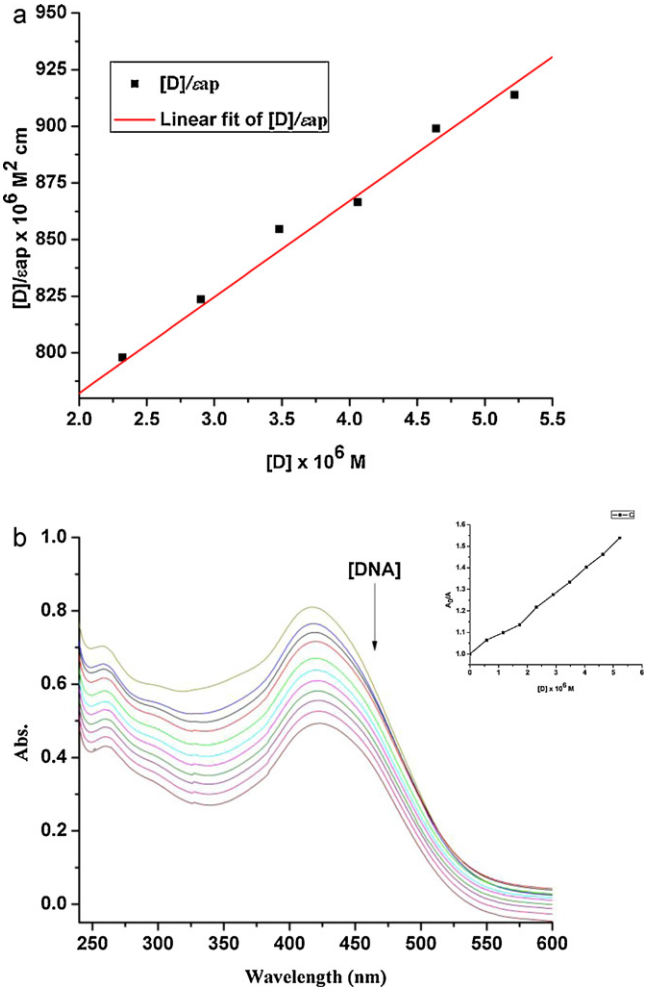

Fig. 6. (a) (AD4), Cu(II)L_1–DNA half-reciprocal plot of D/ε_{ap} vs. D. The binding constant, K_b = (slope/intercept) × 10^6 = 4.67×10^4 M^{-1}. (b) Cu(II)L_1–DNA titration graph of 50 μM of complex in 500 μL of Tris–HCl buffer, 50 mM NaCl, pH 7.32 with *E. coli* plasmid DNA (19.1 ng/μL). DNA titration saturation curve is given in insert.

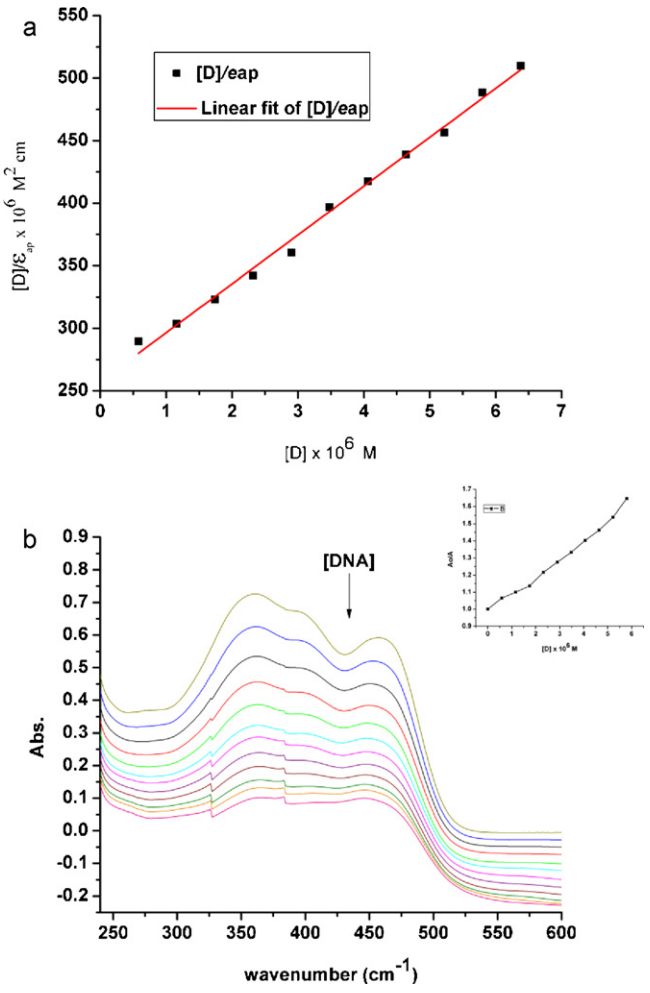

Fig. 7. (a) Zn(II)–L_1–DNA half-reciprocal plot of D/ε_{ap} vs. D. The binding constant, K_b = (slope/intercept) × 10^6 = 1.52×10^5 M^{-1}. (b): Zn(II)–L_1–DNA titration graph of 50 μM of complex in 500 μL of Tris–HCl buffer, 50 mM NaCl, pH 7.32 with *E. coli* plasmid DNA (19.1 ng/μL). DNA titration saturation graph is given in insert.

the complex chromophore with that of DNA bases. That means that Ni(II) complex acts as groove binder with the DNA.

The titration absorption curve for the DNA binding activity with the Co(II)L_1 complex is shown in Fig. 5. There is a hypochromism effect as well as a red-shift at $\lambda = 360\,nm$ ($\Delta\lambda = 6.9\,nm$) with a binding constant of $2.1 \times 10^5\,M^{-1}$ and having isosbestic point at $\lambda = 494.2$. The Co(II) complexes show less affinity towards DNA than the Ni(II) complexes. Complexes of Cu(II) and Zn(II) have much less binding affinity than Ni(II) and Co(II) complexes; they even have different binding modes of interaction or bonding to the DNA. From Fig. 6 for Cu(II) and Fig. 7 for Zn(II) there is no isosbestic point but the absorption bands of chromophores are reduced after addition of DNA which shows the interaction of the complexes' chromophores with DNA bases and their binding with plasmid DNA.

The Ni(II) and Co(II) complexes show better DNA binding activity and interaction than Cu(II) and Zn(II) complexes due to availability of the d-orbital in the case of the Ni(II) and Co(II) complexes. DNA is also acting as a ligand and making binary complexes along with H_2L as different coordinating species and metals are behaving as the central core. In the case of Cu(II) and Zn(II) complexes the ligand chromophores have free coordinating sites even after the coordination with the metal so that their chromophores interact with the DNA.

4. Conclusions

Schiff-base ligand having the coordinating group like CH=N, C=S and =N–NH and their metal(II) complexes have been synthesized and discussed in terms of the spectral as well as physical characterizations. The ligand has the N-containing aromatic rings, and shows positively charged chromophores possibly interacting with the DNA. The DNA interaction study of ligand shows that there was no interaction with the DNA. However, all four synthesized metal(II) Schiff-base complexes with the functional groups like thiocarbohydrazone showed interaction with the DNA by groove binding and intercalation and are supposed to be anticancer agents. The interaction between metal(II) Schiff-base complexes and the DNA is due to the influence of ligand chirality on its DNA binding properties. The Ni(II) and Co(II) complexes show better interaction than Cu(II) and Zn(II) complexes due to the availability of the vacant d-orbital in the case of Ni(II) and Co(II) complexes. In the case of Cu(II) and Zn(II) complexes the ligand chromophores have free coordinating sites even after the coordination with the metal so that their chromophores interact with the DNA. The DNA binding property was a result of the strong stacking interaction between an aromatic chromophore and the base pairs of DNA. Water solubility of the complexes enhanced the biological compatibility of *in vivo* compound activity. The binding constants were found to be in the increasing order of Ni(II) ≥ Co(II) > Zn(II) > Cu(II)> ligand.

Acknowledgements

Financial support from DST/Mintek Nanotechnology Innovation Centre, the National Research Foundation (NRF), Pretoria, South Africa, the University of Johannesburg, and the UJ Commonwealth Fellowship for author Anand D. Tiwari is gratefully acknowledged. Special thanks to the MRDG Department, Indian Institute of Sciences, Bangalore, India, for making available the plasmid genomic *E. coli* DNA.

References

[1] E.M. Hondnett, W.J. Dunn, J. Med. Chem. 13 (1970) 768–770.
[2] E.M. Hondnett, W.J. Dunn, J. Med. Chem. 15 (1972) 339–1339.
[3] J.R. Marrow, K. Kolasa, Inorg. Chim. Acta 195 (1992) 245–248.
[4] K. Sato, M. Chikira, Y. Fuji, A. Kamatsu, J. Chem. Soc. Chem. Commun. (1994) 625–626.
[5] S. Bhattacharya, S.S. Mandal, J. Chem. Soc. Chem. Commun. (1995) 2489–2490.
[6] J. Duguid, V.A. Bloomfield, A.J. Benevides, G.J. Thomas Jr., J. Biophys. 65 (5) (1993) 1916–1928.
[7] A.E. Friedman, C.V. Kumar, N.J. Turro, J.K. Barton, Nucleic Acids Res. 19 (10) (1991) 2595–2602.
[8] A.M. Pyle, T. Morri, J.K. Barton, J. Am. Chem. Soc. 112 (25) (1990) 9432–9434.
[9] A.K. Patara, S. Dhar, M. Nathaji, A.K. Chakravarty, Dalton Trans. 5 (2005) 896–902.
[10] S. Mathur, S. Tabassum, Chem. Biodivers. 3 (2006) 312–325.
[11] S.E. Wolkenberg, D.L. Boger, Chem. Rev. 102 (7) (2002) 2477–2496.
[12] M. Eriksson, M. Leijon, C. Hiort, B. Norden, A. Graslund, Biochemistry 33 (1994) 5031–5040.
[13] I. Haq, P. Lincoln, D. Suh, B. Norden, B.Z. Chawdhary, J.B. Chaires, J. Am. Chem. Soc. 117 (1995) 4788–4796.
[14] J.A. Cowan, Curr. Opin. Chem. Biol. 5 (6) (2001) 634–642.
[15] L.N. Ji, X.H. Zou, J.G. Liu, Coord. Chem. Rev. 216 (2001) 513–536.
[16] J.K. Barton, Science 233 (4765) (1986) 727–734.
[17] C.S. Chow, J.K. Barton, J. Am. Chem. Soc. 112 (7) (1990) 2839–2841.
[18] X. Qu, J.B. Chaires, J. Am. Chem. Soc. 123 (1) (2001) 1–7.
[19] Y. Xiong, L.N. Ji, Coord. Chem. Rev. 185 (1999) 711–733.
[20] M.P. Fitzsimons, J.K. Barton, J. Am. Chem. Soc. 119 (1997) 3379–3380.
[21] P.J. Dandliker, R.E. Holmlin, J.K. Barton, Science 275 (1997) 1465–1468.
[22] A.E. Friedman, J.C. Chambron, J.P. Sauvage, N.J. Turro, J.K. Barton, J. Am. Chem. Soc. 112 (1990) 4960–4962.
[23] D.T. Odom, C.S. Parker, J.K. Barton, Biochemistry 38 (16) (1999) 5155–5163.
[24] W. Xu, F.R. Louka, P.E. Doulain, C.A. Landry, F.A. Mautner, S.S. Massoud, Polyhedron 28 (2009) 1221–1228.
[25] E. Manoj, M.R.P. Karup, H.K. Fun, A. Punnose, Polyhedron 26 (2007) 4451–4462.
[26] M.P. Sathisha, U.N. Shetti, V.K. Revankar, K.S.R. Pai, Eur. J. Med. Chem. 43 (2008) 2338–2347.
[27] W.J. Geary, Coord. Chem. Rev. 7 (1971) 81–122.
[28] A.B.P. Lever, Inorganic Electronic Spectroscopy, 2nd ed., Elsevier, Amsterdam, 1984.
[29] B.J. Hathaway, J. Chem. Soc.: Dalton Trans. 12 (1972) 1196–1199.
[30] R.M. Silvertein, F.X. Webster, Spectroscopic Identification of Organic Compounds, 6th ed., Wiley, New York, 1998, p. 101.
[31] C.C. García, B.N. Brousse, M.J. Carlucci, A.G. Moglioni, M.M. Alho, G.Y. Moltrasio, N.B.D. Accorso, E.B. Damonte, Antivir. Chem. Chemother. 14 (2005) 99–105.
[32] A. Kolocouris, K. Dimas, C. Pannecouque, M. Witvrouw, G.B. Foscolos, G. Stamatiou, G. Fytas, G. Zoidis, N. Kolocouris, G. Andrei, R. Snoeck, E. De Clercq, Bioorg. Med. Chem. Lett. 12 (5) (2002) 723–727.
[33] K. Nakamoto, Infrared and Raman Spectra of Inorganic and Coordination Compounds, 4th ed., Wiley, New York, 1986, p. 242.
[34] C.Y. Zhong, J. Zhao, Y.B. Wu, C.X. Yin, P. Yang, J. Inorg. Biochem. 101 (2007) 10–18.
[35] M.A. Pyle, P.J. Rehmann, R. Meshoyrer, J.N. Kumar, J.N. Turro, K.J. Barton, J. Am. Chem. Soc. 111 (1989) 3051–3058.